SUPPLMENTARY MATERIAL

Cell Surface Glycan Engineering of Neural Stem Cells Augments Neurotropism and Improves Recovery in a Murine Model of Multiple Sclerosis

Jasmeen S. Merzaban, Jaime Imitola, Sarah C. Starossom, Bing Zhu, Yue Wang, Jack Lee, Amal J. Ali, Marta Olah, Ayman F. Abuelela, Samia J. Khoury and Robert Sackstein

FIGURE LEGENDS

Supplementary Figure 1: Inflammatory cytokine treatment does not induce selectin ligand expression on mouse NSCs. NSCs were stimulated with 10 ng/ml of TNFα, 10 ng/ml IL-1β, 10 ng/ml IFNγ independently or in combination (all at 10 ng/ml). At 24 h, NSCs were harvested and analyzed by flow cytometry for E-selectin binding. Controls included untreated NSCs and Kg1a cells (positive control for E-selectin binding).

Supplementary Figure 2: α1,3-fucosyltransferase expression in mouse neurospheres isolated from the telencephalic ventricular zone of murine embryonic day 11.5 determined from expression array data set (GSE10796 (Sanosaka, T., Namihira, M., et al. 2008)). Solid line represents the median expression of all the genes assessed while dotted lines represent 25 and 75 percentile expression value for all the genes assessed. FTXI and FTIX are significantly expressed (FDR = 0.016 and FDR < 0.05 respectively). FTX is moderately expressed (FDR < 0.05) while FTIV and FTVII are insignificantly different from zero expression. Student's t-test (one-sample,

one-tailed hypothesis) was performed. *P*-value adjustment was performed using FDR (Benjamini Hochberg) method. * $p < 0.05$ and ** $p < 0.02$.

Supplementary Figure 3: HCELL and NCAM are the major E-selectin ligands identified on NSCs following GPS treatment. Whole cell lysates of mouse NSCs were initially immunoprecipitated using mAb directed to CD44 (included in **Figure 3A**); the residual lysate was then exhaustively immunoprecipitated with anti-CD56 (NCAM) mAb for 3 rounds (lanes 1, 2, 3). A very weak E-Ig reactivity after exhaustive immunoprecipitation remains (lane 4; possibly residual CD44 based on the size).

Supplementary Figure 4: HCELL is the only E-selectin ligand created by GPS treatment of CC-2599 human NSCs. **(A)** Flow cytometric analysis of CD15, CSLEX-1, HECA452, and E-selectin ligand (E-Ig binding), expression on human NSCs either treated with GPS (grey bars) or buffer-treated (BT; black bars). The mean fluorescence intensity is shown for each antibody measured. **(B)** Flow cytometric analysis of CD44, PSGL-1, NCAM, and CD43. **(C)** Western blot analysis of E-Ig reactivity to human NSC lysates. CD44 and NCAM were immunoprecipitated from equivalent amounts of cell lysates from GPS-treated (+) or buffer-treated (-) human NSCs. Immunoprecipitates were then electrophoresed and blotted with E-Ig. Staining of GPS-treated NSCs with E-Ig was performed in the presence of Ca^{2+}.

Supplementary Figure 5: GPS treatment does not affect of the ability of NSCs to form neurospheres. 200 viable GFP^{+} NSCs were plated per well in a 96 well plate immediately following GPS treatment for 7 days. The resulting neurospheres were counted and neurosphere

frequency was calculated as the number of neurospheres divided by number of cells plated. There was no statistically significant difference in the density of neurospheres or the number of neurospheres formed between BT-NSCs and GPS-NSCs. A representative image of the GFP^+ neurospheres used for these experiments is shown where the red fluorescence indicates Nestin expression and the green fluorescence indicates GFP. Note that BT- and GPS-GFP^+ NSCs were both able to form neurospheres equally. This figure is related to **Fig. 3** in the main text.

Supplementary Figure 6: GPS treatment does not affect the differentiation capacity of NSCs into neurons **(A)**, astrocytes **(B, D)** or oligodendrocyte precursors **(C, D)**. $1x10^5$ BT- and GPS-NSC were cultured in the appropriate differentiation media and after 120 hours, numbers of MAP-2^+ neurons **(A)**, $GFAP^+$ astrocytes **(B, D)**, and $NG2^+$ oligodendrocytes **(C)** were counted per 20x vision field. There was no statistically significant difference between the ability of BT and GPS-NSCs to differentiate along these three lineages (p=0.1). **(D)** $GFAP^+$ astrocytes and $NG2^+$ oligodendrocytes are shown in red and To-Pro3 is used to stain nuclei of neural stem cells treated in vitro with control buffer (BT) or FTVI (GPS). Scale bar, 50μm. This figure is related to **Fig. 3** in the main text.

Supplementary Figure 7: GPS treatment does not affect the immunomodulation function of NSCs in vitro. Direct *in vitro* suppressive effects of NSCs on lymph node cells (LNCs) were measured by coculturing irradiated NSCs with LNCs isolated from naïve C57BL/6 mice. Both irradiated BT-NSC and GPS-NSC suppressed ^{3}H-thymidine incorporation **(A)** into LNCs in response to concanavalin A (ConA) in a dose-dependent manner and also suppress inflammatory

cytokine production **(B)** as measured by ELISA to an equal degree; the ratios correspond to numbers of NSCs to numbers of LNCs (1:4, 1:2, 1:1, 2:1, and 4:1).

Note that by increasing the ratio of NSC:LNC compared to LNC alone (first bar), the amount of ^{3}H-thymidine incorporation decreased significantly (p=0.0005). Also note that there was no statistically significant difference between the ability of BT-NSC (white bars) and GPS-NSC (gray bars) to inhibit proliferation (p=0.2). **(C)** 1x10^{6} BT-NSCs or GPS-NSCs were treated for 24 h with or without inflammatory cytokines (10ng/mL IFN-ϒ and 15ng/mL TNF- α) and with or without E-Ig (5ng/mL) prior to RNA extraction and cDNA synthesis. Real-time RT-PCR revealed the fold change in gene expression (related to BT or GPS-NSCs alone) calculated using $2^{-\Delta\Delta CT}$ method and the relative expression of LIF mRNA was assayed relative to GAPDH housekeeping gene. Values are means ± SEM (n = 4 experiments). This figure is related to **Fig. 3** in the main text.

Supplementary Figure 8: GPS-NSCs migrate to the CNS parenchyma more efficiently than BT-NSCs. 1 x 10^{6} GPS-NSCs or BT-NSCs were labeled with PKH26 dye and were injected intravenously to MOG-induced EAE mice on day 9 and day 13 post-immunization (PI). Brains were harvested on day 17 PI and snap-frozen before 20μm sections were prepared and stained with antibodies: anti-Flk-1 (VEGFR2; green) or anti-SOX-2 (red) to reveal blood vessels and the position of the NSCs respectively. **(A)** BT NSCs are primarily localized with FLK-1^{+} endothelial cells whereas GPS-NSCs are found in the parenchyma as they have crossed the endothelium. These NSCs express sox-2, a marker for neural stem cells **(B)**. This figure is related to **Fig. 5** in the main text.

Supplementary Figure 9: GPS treatment generates robust E-selectin ligand activity on mouse HSPCs but this does not translate into amelioration of EAE. **(A)** Flow cytometric analysis of E-Ig reactivity on BT- and GPS- mouse hematopoietic stem/progenitor cells (HSPC; Lineage^{neg}C-kit^{pos}). The mean fluorescence intensity is shown above each histogram for the $hIgG_1$ isotype control, E-Ig reactivity on BT-HSPC and E-Ig reactivity on GPS-HSPC. These cells were used for in vivo EAE experiments as a control. **(B)** The EAE clinical scores in C57BL/6 mice immunized with MOG 35-55 on Day 0 and subsequently injected with $1x10^6$ buffer-treated HSPC (BT-HSPC; open blue diamonds; n = 30), GPS-treated HSPC (GPS-HSPC; open purple diamonds; n = 30) or sham-treated mice (No NSC; filled black circles; n = 30) on day 9 and day 13 after immunization were determined. No significant improvement in the clinical scores was evident in mice receiving either BT- or GPS-HSPC. **(C)** The cumulative burden of disease was assessed by performing a linear regression analysis comparing the slope of the curves in **(B)**. This figure is related to **Fig. 6** in the main text.

Supplementary Figure 10: No evidence of GFP signal was observed at Day 30 PI from either BT- or GPS- NSCs injected into EAE mice.

C57BL/6 Mice were sacrificed 30 days after immunization with MOG 35-55 (on day 0) and subsequent injection with $1x10^6$ buffer-treated NSCs (BT-NSC), GPS-treated NSCs (GPS-NSC) or sham-treated mice (No NSC) on day 9 and day 13 and immunohistochemistry for GFP^+ cells was performed. At 30 days PI GFP^+ cells were not identified in sections of relevant study groups, even when antibodies against GFP (red) were compared to endogenous GFP signal (EGFP; green). Cultured NSCs before injection were used as a positive control (NSC-Pre Tx) and showed a robust GFP signal. Scale bar, 50μm. Data here is related to **Fig. 6**.

Supplementary Figure 11: Model of neurorestoration afforded by GPS treatment of native-NSCs surface proteins, CD44 and NCAM, creating novel step 1 effectors, HCELL and NCAM-E, that efficiently bind endothelial E-selectin in EAE mice. As a result of injury, endothelial cells and glia may produce injury signals (e.g., SDF-1α and E-selectin) that direct GPS-NSCs toward the injury-induced niches in higher number than in control mice. Despite the increased number of NSCs recruited, instead of cell replacement, NSCs offer local modulation of immunity and endogenous regeneration of CNS by increasing the number of SOX-9^{+}/Olig-2^{+} oligodendroglia. This subsequently leads to more mature oligodendroglial cells (CNPase^{+}), less axonal loss, and more axonal regeneration. Niche molecules secreted by primitive neural stem cells may promote some of the effects provided by their increased colonization.

Supplementary Table I. EAE features in C57BL/6 mice treated intravenously with GPS treated HSPCs Details of the clinical scores of EAE mice receiving HSPCs compared to sham-control are show.

Sanosaka T, Namihira M, Asano H, Kohyama J, Aisaki K, Igarashi K, Kanno J, Nakashima K. 2008. Identification of genes that restrict astrocyte differentiation of midgestational neural precursor cells. *Neuroscience*, 155:780-788.

Supplementary Figure 1

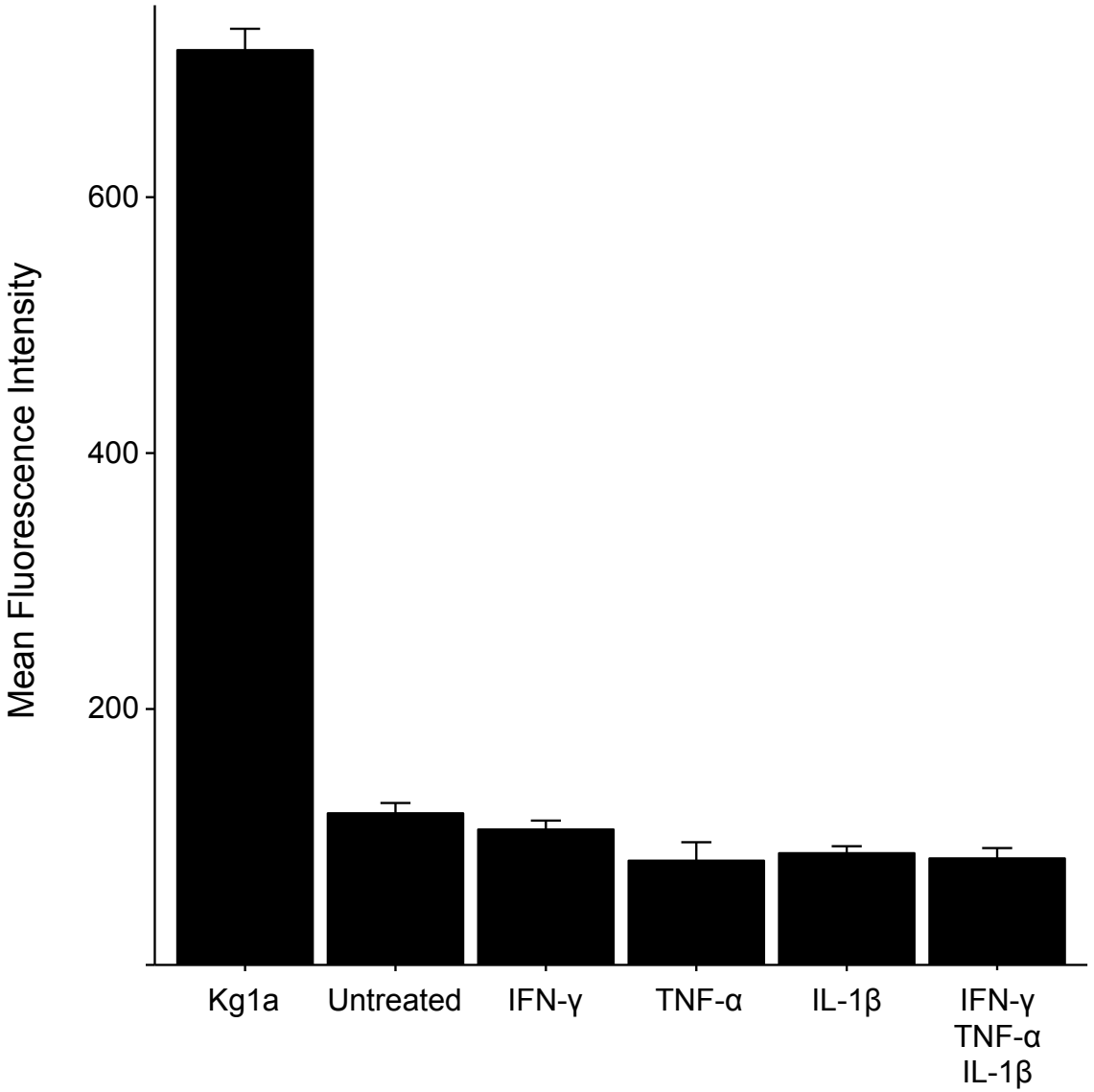

Supplementary Figure 2

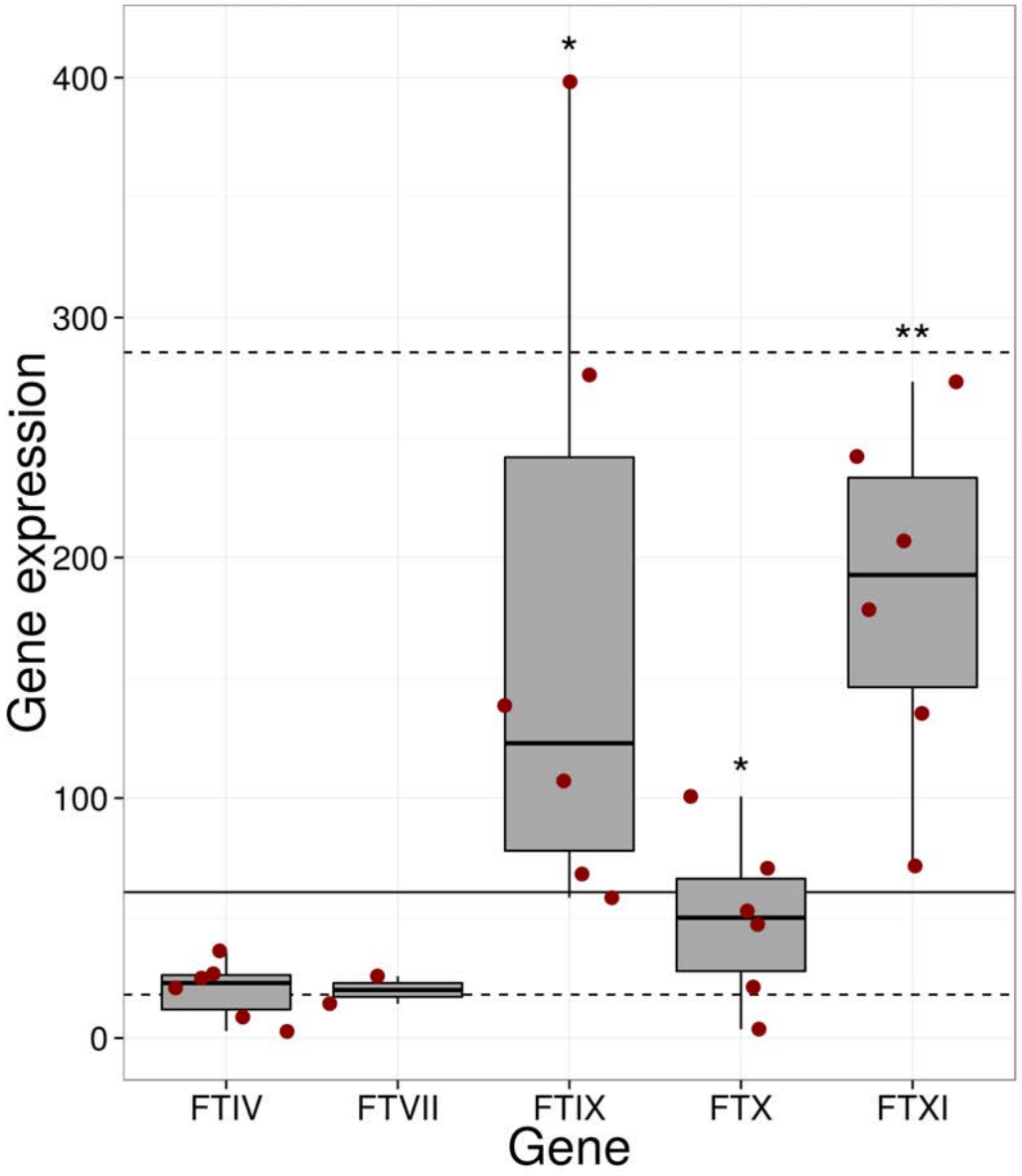

Supplementary Figure 3

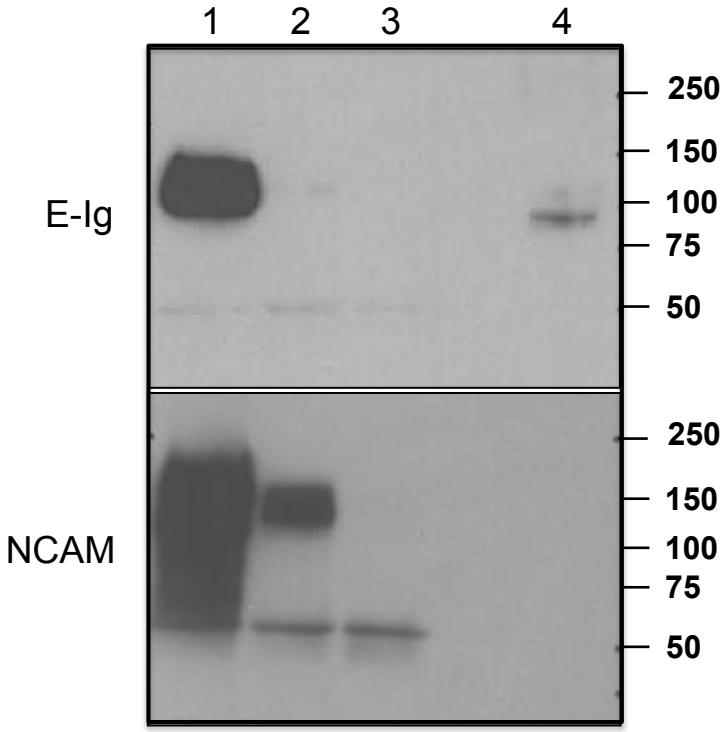

Supplementary Figure 4

A

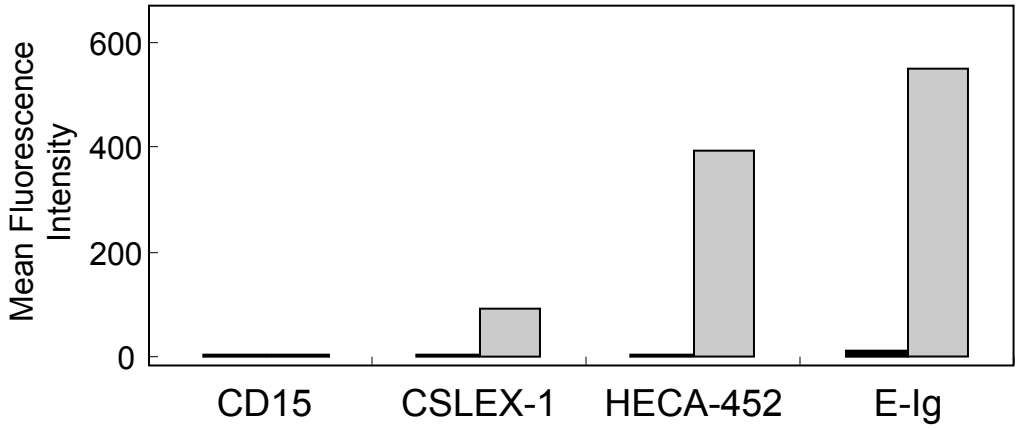

B

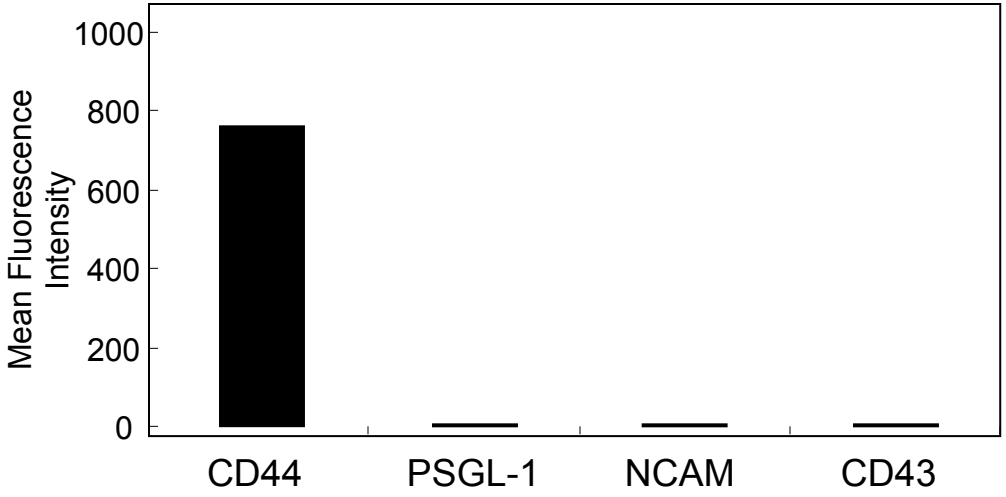

C

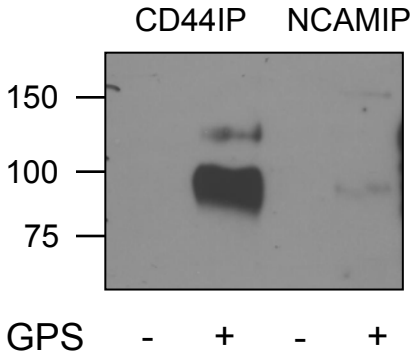

Supplementary Figure 5

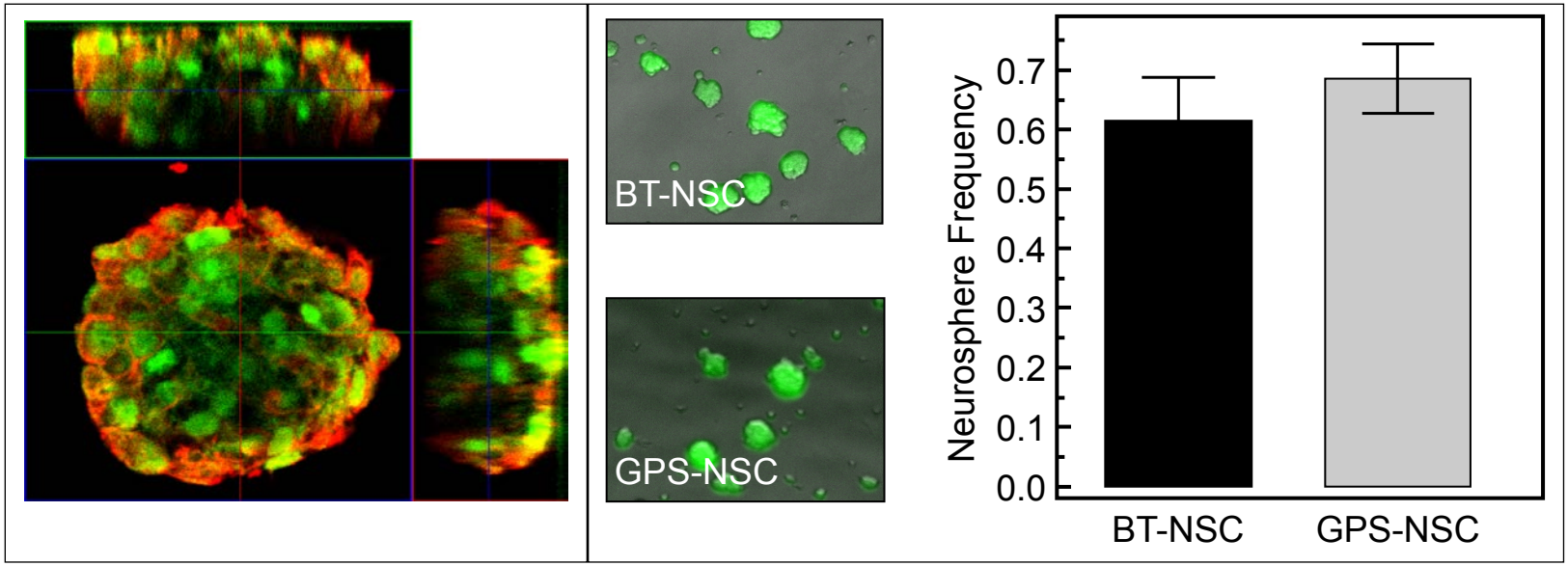

Supplementary Figure 6

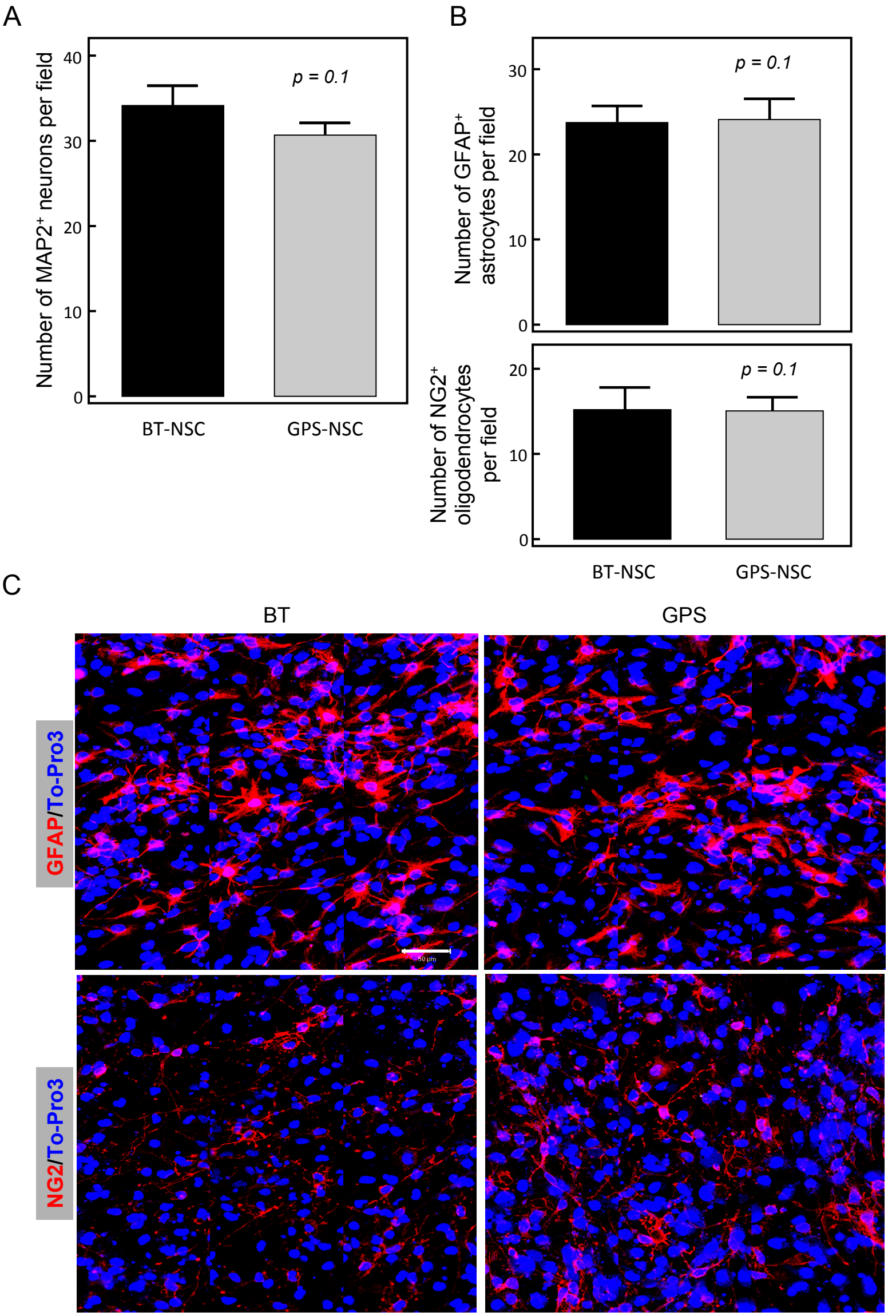

Supplementary Figure 7

A

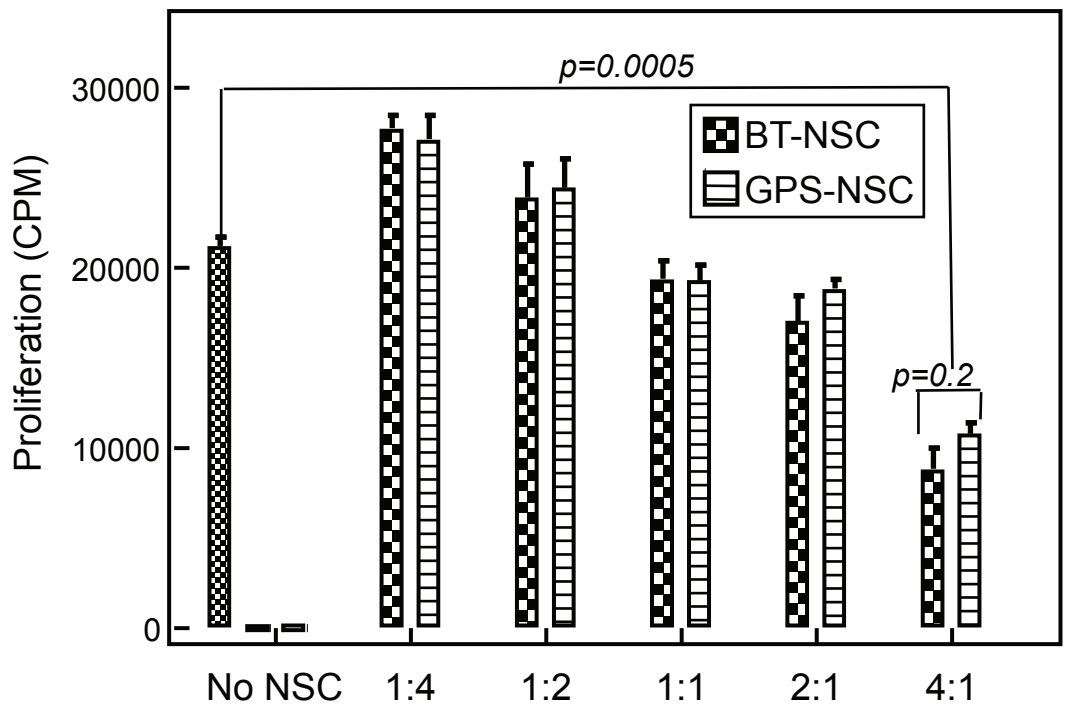

B

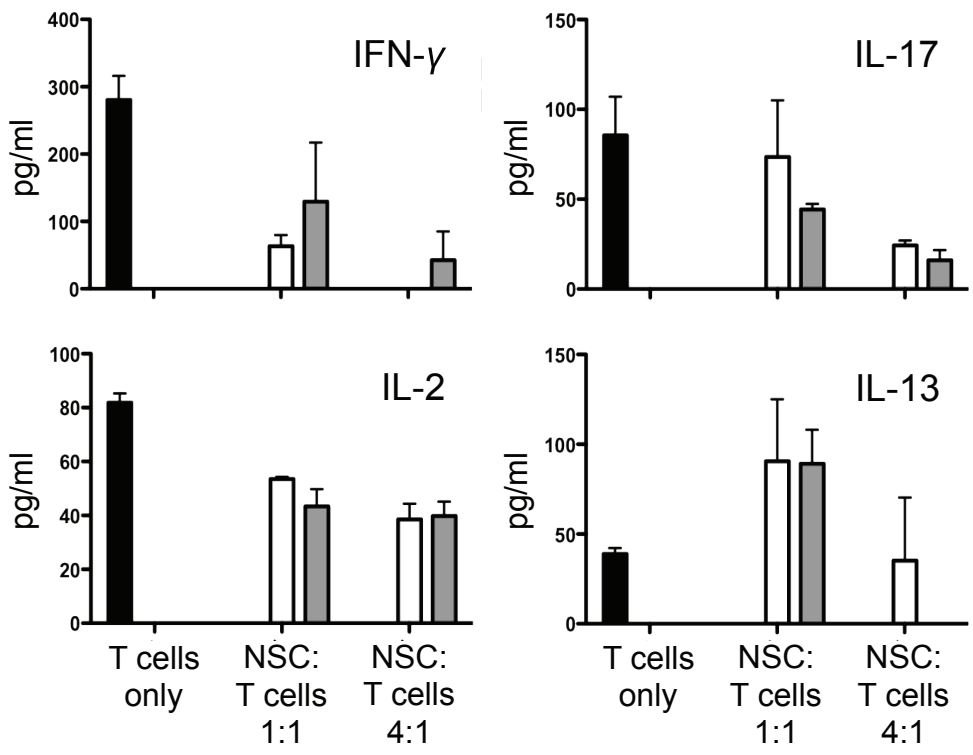

C

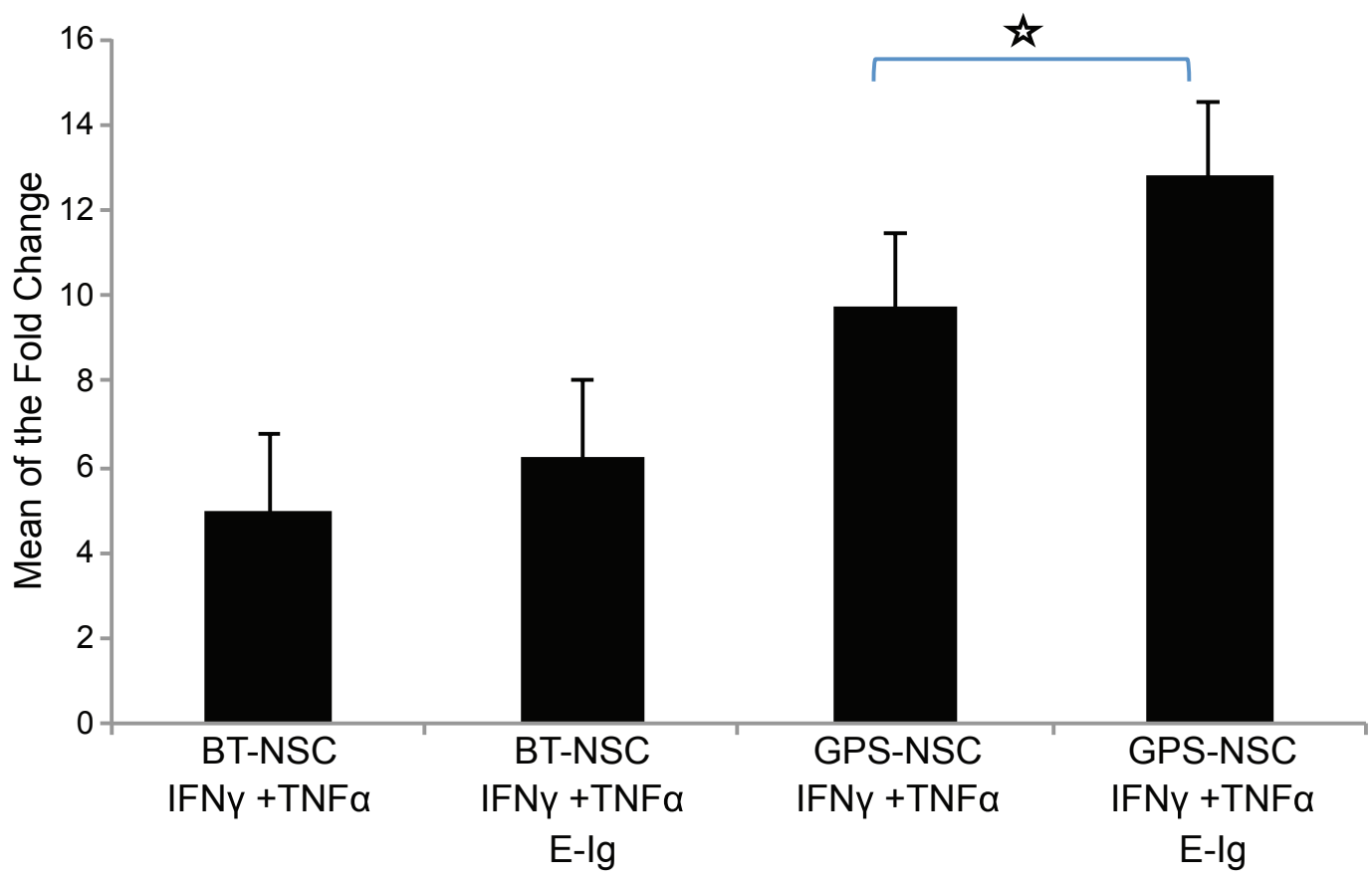

Supplementary Figure 8

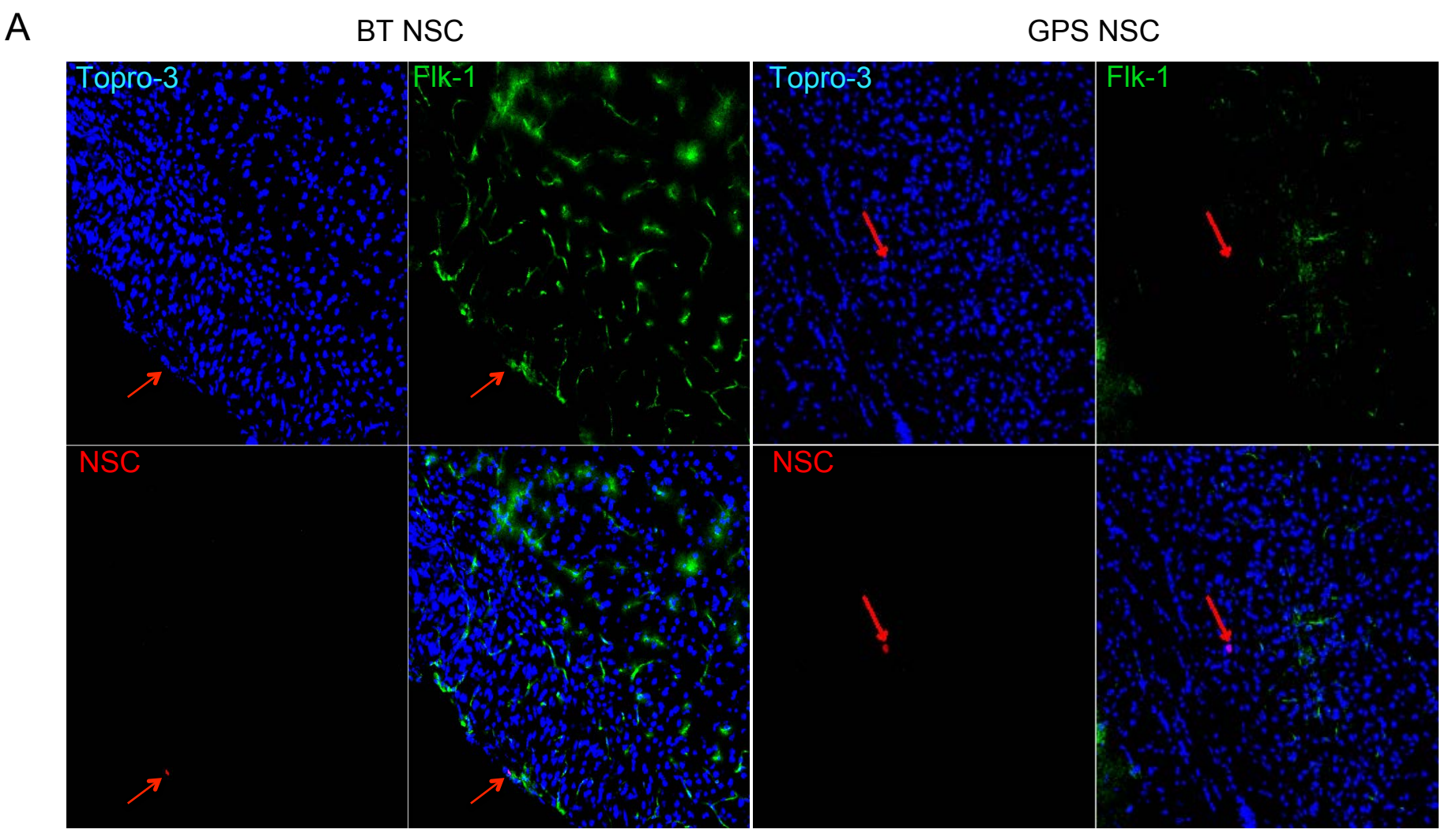

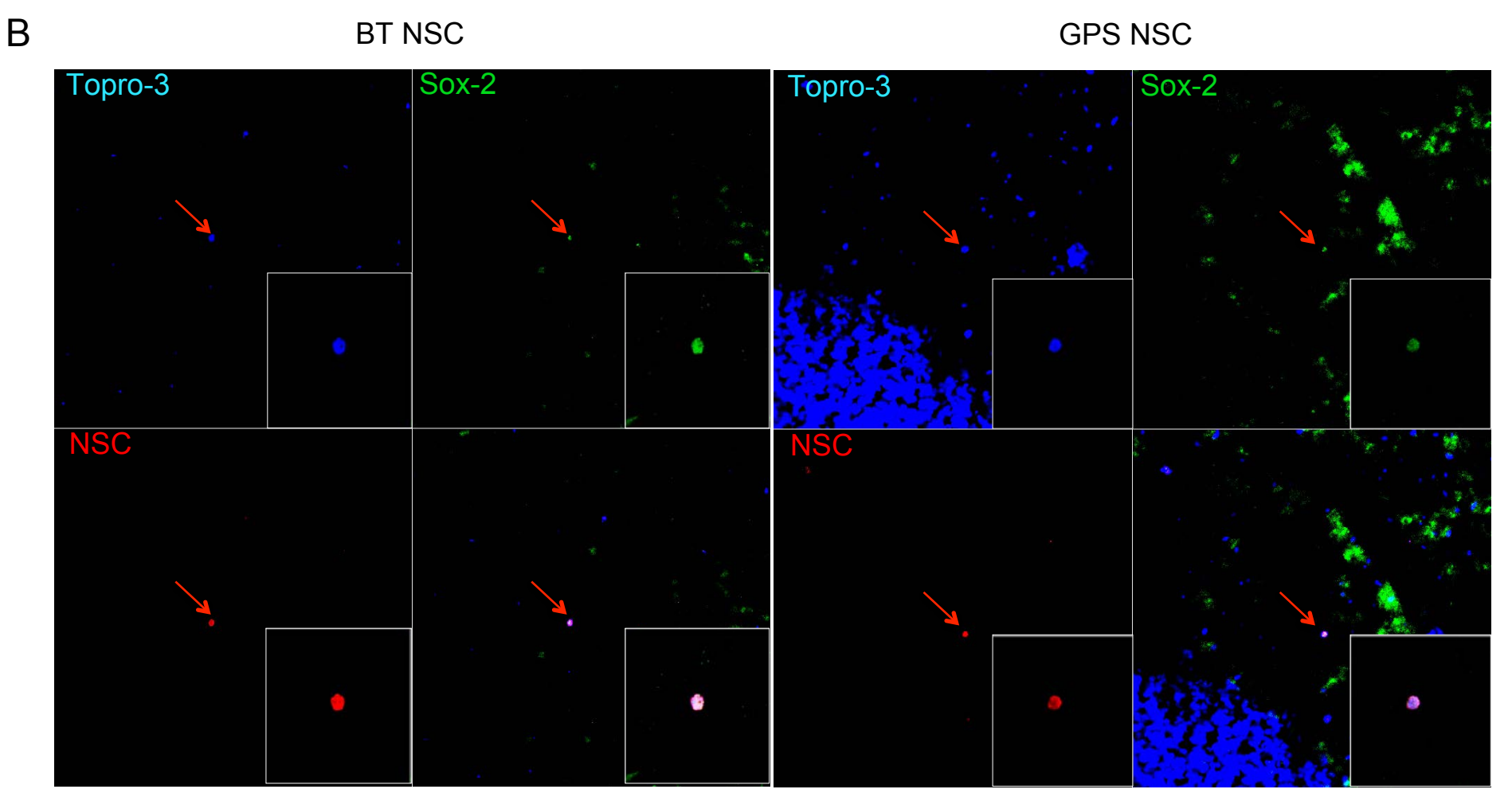

Supplementary Figure 9

A

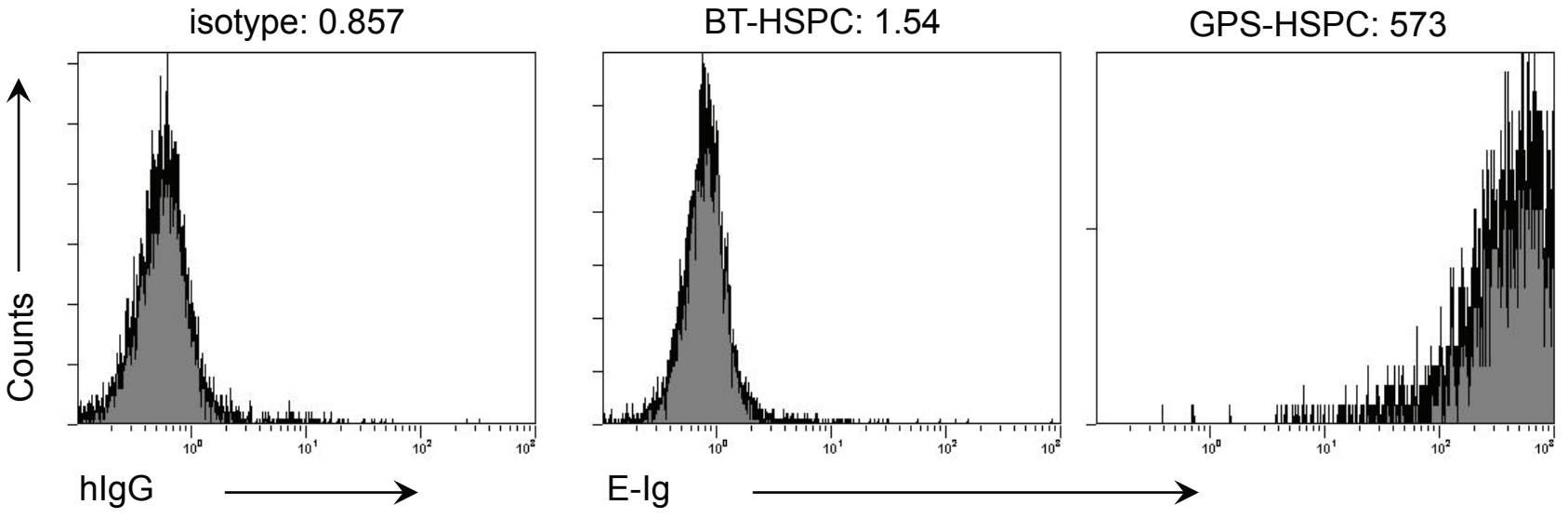

B

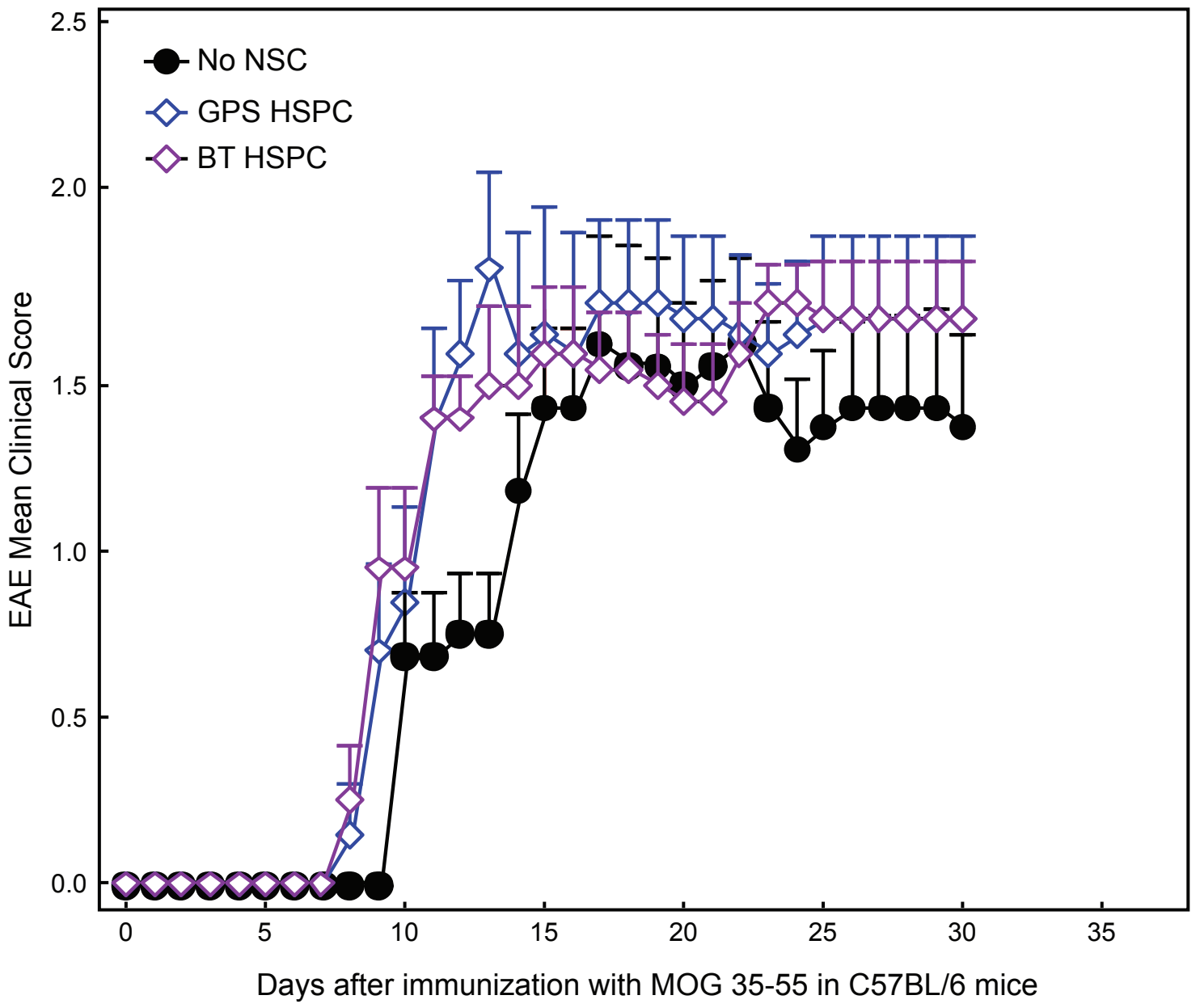

C

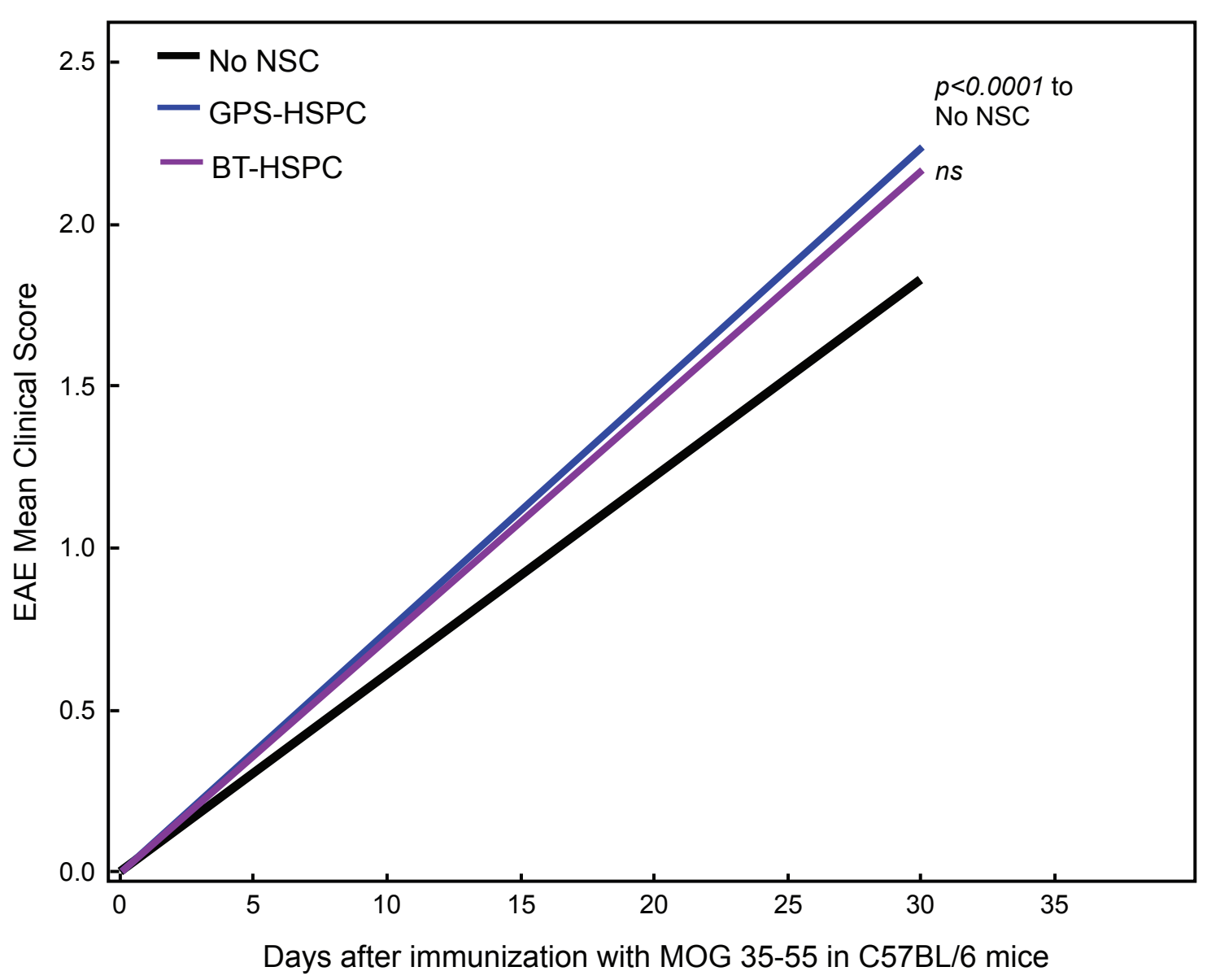

Supplementary Figure 10

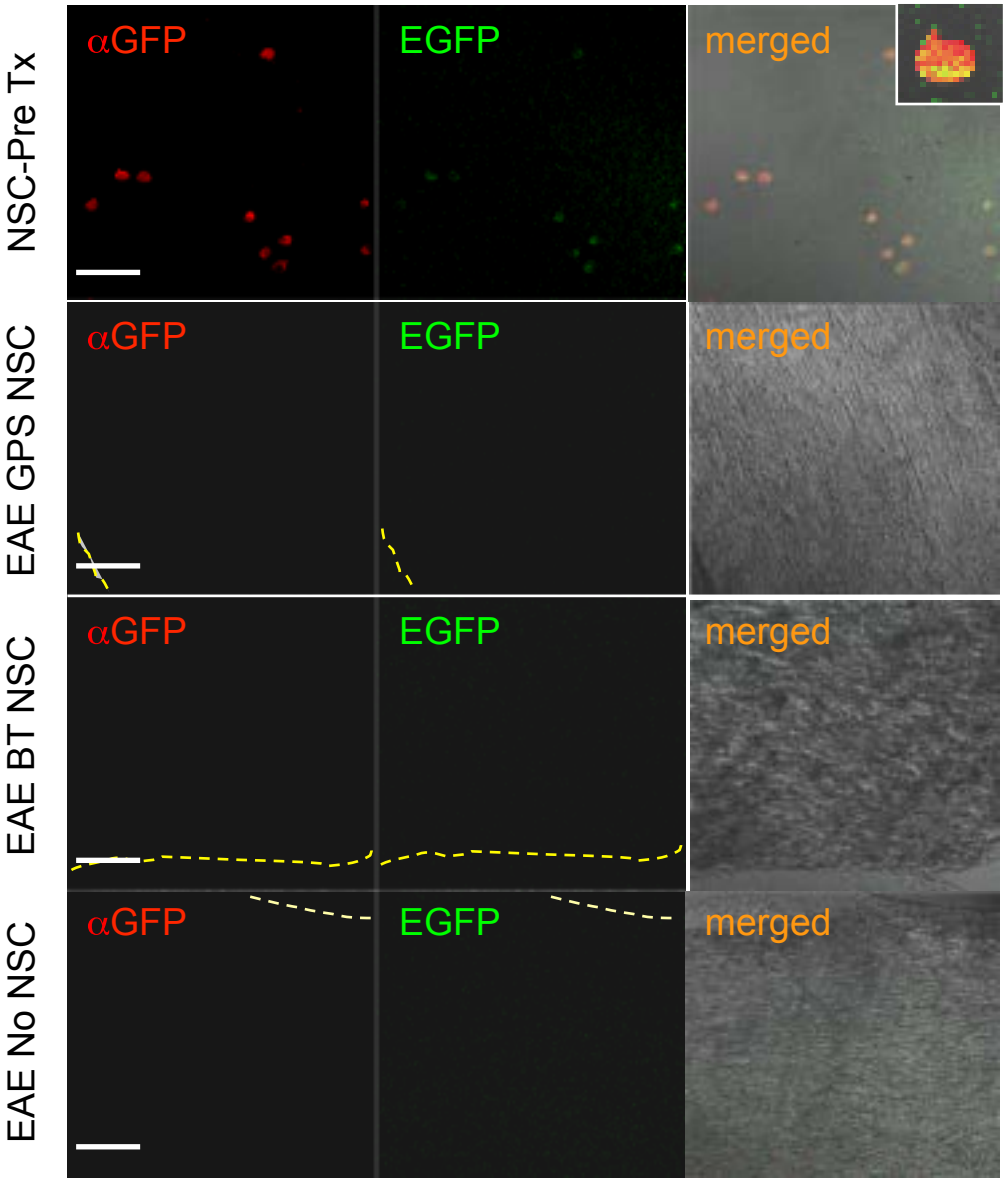

Supplementary Figure 11

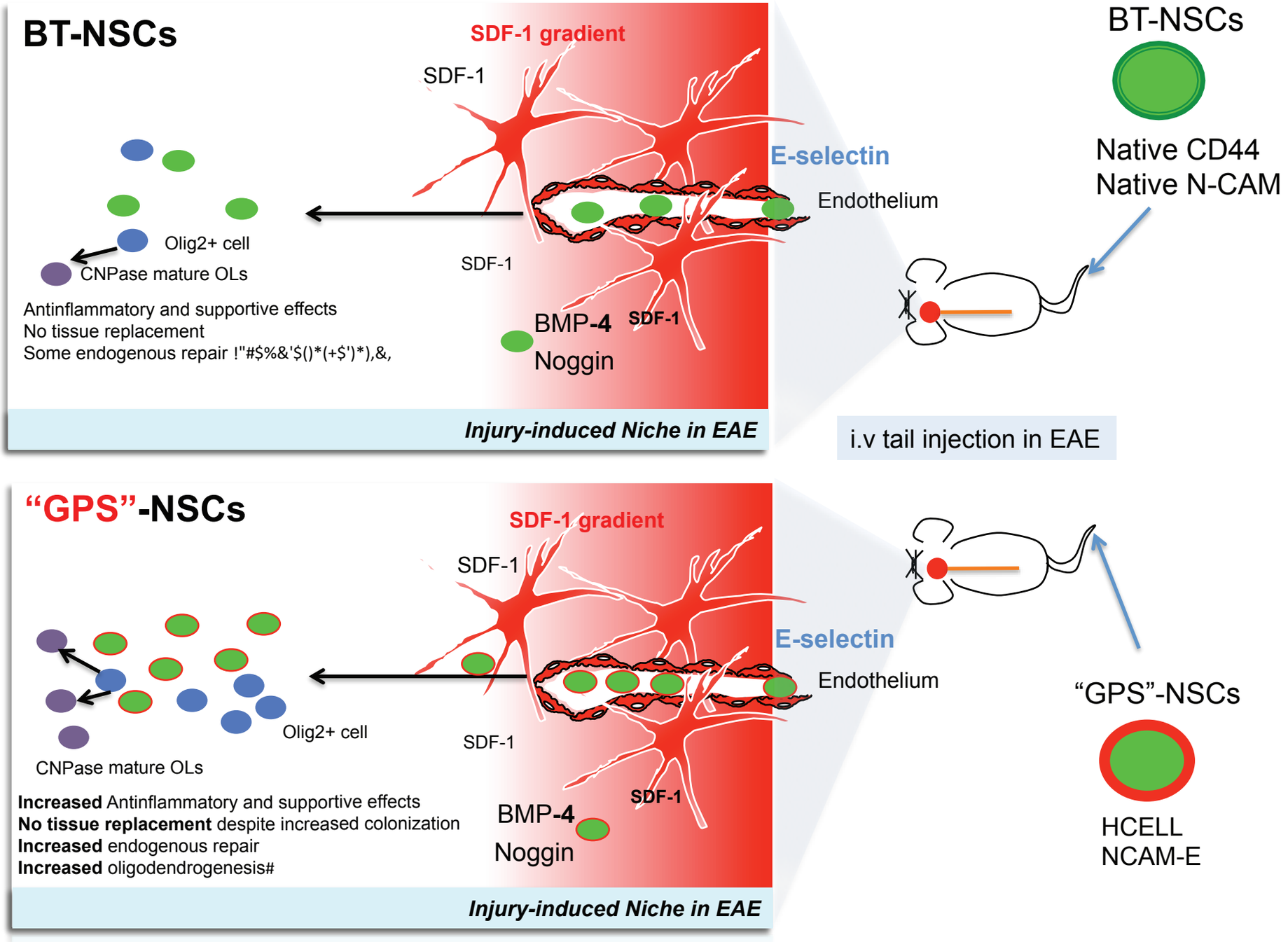

Supplementary Table 1

EAE clinical features in C57BL/6 mice injected with i.v. GPS treated HSPCs.

Treatment	Route of cell administration	No. of mice	Disease onset (days p.i)	Maximum clinical score	Cumulative disease score (0-20 p.i)	Cumulative disease score (21-30 p.i)
No Cells	-	30	13.22±0.6	2.2±0.4	15.75±0.6	14.9±2.4
BT-HSPC	i.v	30	10±0.7	2.1±0.2	17.2±1*	16.7±1*
GPS-HSPC	i.v	30	9.5±0.4	2.5±0.6	18.3±2.2**	16.8±1.7*

* $p<0.05$ ANOVA multiple comparisons.